JOURNAL OF CATALYSIS 69, 454–464 (1981)

Surface Characterization of Supported Pt–Pd Bimetallic Clusters Using Infrared Spectroscopy

CHARLES M. GRILL, MARY L. MCLAUGHLIN, JAMES M. STEVENSON, AND RICHARD D. GONZALEZ[1]

Department of Chemistry, University of Rhode Island, Kingston, Rhode Island 02881

Received September 25, 1980; revised January 5, 1981

The chemisorption of CO on a series of silica-supported Pt–Pd bimetallic samples has been studied. Using simple mathematical arguments to relate the absorbances of CO adsorbed on Pt and on Pd to metal compositions, we find no evidence of surface enrichment of either metal. Measurements of the H_2/CO uptake ratio suggest that bimetallic-cluster formation inhibits H_2 absorption. Exposure to oxygen followed by rereduction in hydrogen results in the formation of Pd-rich particles, as evidenced by an increase in hydrogen adsorption. Using a theory originally developed by Sachtler, we find that the decrease in intensity of the bridged Pd–CO bands relative to the linear Pd–CO bands may be due not only to geometric effects (including short-range ordering), but also to a ligand effect. Most bands in the bimetallic systems are also shifted to lower frequencies. This is another ligand effect and may be explained by the coherent potential theory of alloy formation.

INTRODUCTION

The possible preferential surface enrichment by one of the metallic components in either an alloy or a supported bimetallic cluster has attracted a great deal of attention over the last few years. With the development of modern sophisticated instrumentation, progress in this area has been very impressive. Techniques such as ESCA, SIMS, ISS, EXAFS, and AES have enabled investigators to obtain reasonably good estimates of surface compositions (*1*). All of these instrumental techniques are subject to the following limitations: (1) they require the use of high vacuums, or moderately high vacuums in the case of ESCA, and cannot be used under reaction conditions where significant surface reconstruction may occur; (2) they are expensive and not accessible to the average surface chemistry laboratory; and, (3) with the possible exception of ISS, they do not sample the uppermost layer. If one considers that finely dispersed metal particles can be in the neighborhood of 10–20 Å, it is evident that analysis by either AES or ESCA yields an analysis of the bulk composition since one is essentially studying the entire sample.

If these electron spectroscopic techniques are excluded, one is inevitably left with infrared spectroscopy and selective chemisorption. Infrared spectroscopy has several distinct advantages over electron spectroscopic techniques but also presents certain limitations. The most obvious advantages of infrared spectroscopy are: (1) surface compositions may be studied under reaction conditions; (2) only the uppermost layer is sampled; (3) considerably more chemical information regarding the disposition of atoms within the surface layer is obtained; and (4) the method is inexpensive and simple to use. Disadvantages include: (1) the necessity for extensive preliminary experiments on each bimetallic cluster system; and (2) a reduction in the degree of accuracy.

Recently in this laboratory (*2*), the surface characterization of a series of silica supported Pt–Ru samples was successfully accomplished using a combination of selec-

---

[1] To whom correspondence should be addressed.

0021-9517/81/060454-11$02.00/0

tive chemisorption and infrared spectroscopy. When a mixture of CO and NO was contacted with a silica-supported Pt–Ru bimetallic sample, NO was selectively chemisorbed on Ru surface sites, while CO was selectively adsorbed on the Pt surface sites. The chemisorbed layer formed in this manner was stable provided that excess NO(g) was evacuated from the system as a slow reaction between NO(g) and CO(ads) was observed. Upon measuring the relative adsorbances of CO(ads) and NO(ads), and by applying a simple mathematical argument, surface enrichment in either metallic component was not detected.

In an effort to extend this technique to other bimetallic systems, we performed a preliminary investigation on the silica-supported Pt–Pd system (*3*). In this study, we found that neither CO nor NO was selectively chemisorbed on Pd in the presence of the other. In both cases a chemical reaction between CO and NO occurred rather than a simple displacement of one adsorbed species by the other. These conclusions were based on analysis of the gas phase which showed that large amounts of N_2O and CO_2 were present.

Although neither CO nor NO was selectively chemisorbed on Pd, it still seemed possible to use selective chemisorption to characterize the surface composition of silica-supported Pt–Pd bimetallic clusters. Since CO was selectively chemisorbed on Pt in the presence of adsorbed NO (there is a slow reaction between NO(g) and CO(ads)), the following experiment seemed reasonable: Adsorb CO onto the Pt–Pd sample, saturating both Pt and Pd surface sites with CO. The addition of NO(g) to the system should then result in the replacement of CO by NO on Pd surface sites but not on the Pt surface sites, where it is more strongly adsorbed. A characterization study similar to that reported by Ramamoorthy and Gonzalez (*2*) should then be possible.

The results of this experiment have been reported in another study (*4*). This procedure was untenable for two reasons. First, when NO was added to a silica-supported Pt–Pd sample (atomic ratio, 1 : 1.1) the CO was not only displaced from the Pd, but much of the CO adsorbed on the Pt reacted with NO(g). When CO(g) was back added to resaturate the Pt surface sites, there was a reaction between CO(g) and the NO adsorbed on the Pd surface sites. Second, evidence was found that this procedure induced segregation of the bimetallic clusters in Pt- and Pd-rich particles. A similar segregation effect was also observed when the Pd–Pt bimetallic clusters were alternatively exposed to oxidation–reduction cycles. Such a gross reconstruction of the surface would, of course, invalidate any results obtained.

In view of the particle segregation effects observed in an oxidizing atmosphere, we decided to pursue these surface characterization studies from a different perspective. CO linearly adsorbed on Pt is much more strongly held than CO linearly adsorbed on Pd (*3, 5, 7*). Although the absorption frequencies of these two species are close to one another, it is still possible to determine the intensity of each band. The absorbance of CO linearly adsorbed on Pd may be found by measuring the absorbance at the characteristic frequency at full surface coverage, and again, following evacuation. The difference between the two spectra is calculated. The absorbance of CO linearly adsorbed on Pt is measured at the lower pressure. Since bridge-bonded CO does not occur on silica-supported Pt (*7, 8*), the bands below 2000 cm^{-1} are due solely to CO bridge-bonded to Pd.

When Pd and Pt are alloyed, it is found that the intensity of the bridged Pd–CO bands relative to the linear Pd–CO bands is decreased. The geometric effect of diluting the number of adsorption sites which contain adjacent Pd atoms is a major reason for this observation. A similar result was reported by Soma-Noto and Sachtler (*9*) on a series of supported Pd–Ag samples. Using arguments similar to those employed by

Sachtler (*10*), we also found a ligand effect favoring the linear Pd–CO species.

In order to obtain approximate dispersions and to verify whether a true Pt–Pd bimetallic cluster was formed, chemisorption measurements were carried out. Since Pd particles tend to absorb as well as adsorb hydrogen, a high H_2/CO ratio should be indicative of the formation of separate Pt- and Pd-rich particles.

EXPERIMENTAL

All bimetallic samples had a total loading on silica of about 6% and were prepared as follows: $PdCl_2$ (Ventron Alfa Products, Beverly, Mass.) was dissolved by adding concentrated HCl to a suspension of $PdCl_2$ in H_2O which was maintained at 60°C. Under these conditions, soluble $PdCl_4^{2-}$ was formed. The solution prepared in this way was mixed with another solution which contained a measured amount of $H_2PtCl_6 \cdot 6H_2O$ (Strem Chemical, Boston, Mass.). A slurry was then formed by adding the above solution to Cab-O-Sil, Grade M-5 (Cabot Corp., Boston, Mass.). The slurry was air dried at room temperature for about 1 week, stirring regularly to retain uniformity. The dried catalyst was ground into a fine powder, less than 45 μm, and pressed into self-supporting disks 25 mm in diameter and having a thickness of 16 mg/cm^2. One of the disks was placed in a stainless steel sample holder and suspended by a stainless steel wire in the infrared cell. The cell was similar in design to that of Brown and Gonzalez (*11*) and later refined by Ramamoorthy, *et al.* (*12*).

The gases used in this study were purified as follows: CO (Matheson research grade) was passed through a liquid N_2 trap. Commercial H_2 (Cranston Welding Supplies), used in the reduction of the samples, was first passed through a Deoxo unit to convert O_2 impurities to H_2O. The H_2O was then removed by a molecular sieve backed by a liquid N_2 trap. The purity of all gases was checked periodically on a Dupont Model-104 mass spectrometer.

The sample disks were reduced according to the following procedure: evacuated for 1 hr at 350°C, reduced in flowing H_2 at 350°C for 6 hr, and evacuated for 2 hr at 350°C. The sample was then cooled to room temperature and the evacuation continued until the final pressure was about 10^{-6} Torr (1 Torr = 133.3 Nm^{-2}).

The cell was then transferred to the infrared spectrometer and connected to a Pyrex vacuum system. From this system, gases could be added or evacuated from the cell. All spectra, with the exception of those shown in Fig. 1 were recorded on a Perkin–Elmer Model 281 infrared spectrometer. The spectra shown in Fig. 1 were obtained on a Perkin–Elmer Model 521 infrared spectrometer. The double-beam method was used in all cases. In this method, disks are placed in both the sample and reference beams. The absorption bands due to silica are thus canceled and a relatively flat baseline is obtained.

Chemisorption measurements were performed in a standard volumetric system equipped with a gas burette. H_2 uptake including both adsorption and absorption (β phase hydride formation) was obtained by measuring the total uptake at a H_2 pressure

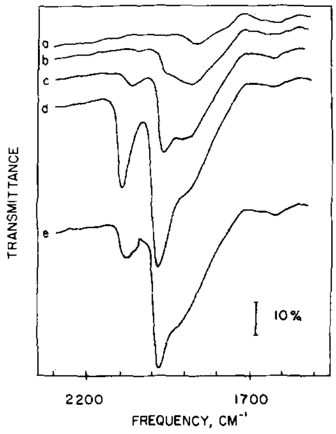

FIG. 1. Stepwise adsorption of CO on 5% silica-supported Pd. (a) Background. (b) First addition of CO. (c) Second addition of CO. (d) Final addition of CO. Pressure ≈10 Torr. (e) 15-min evacuation. Pressure ≈10^{-2} Torr.

of 100 Torr. No attempt was made to distinguish between adsorption and absorption in this study, as standard techniques used by other investigators on Pd (*13*, *14*) fail when applied to H_2 uptake on bimetallic clusters. CO adsorption isotherms were relatively flat so that CO adsorption was taken as the total uptake at a CO pressure of 50 Torr. Pretreatment of the samples prior to the adsorption measurements was identical to that followed in the infrared studies.

RESULTS AND DISCUSSION

Adsorption Measurements

The adsorption of CO and H_2 on a series of silica-supported Pt–Pd bimetallic clusters was studied in order to: (1) explore the effect of clustering on the absorption of H_2 on Pd, and (2) to estimate the effect of clustering on dispersion. The results are shown in Table 1. It is clear from the data that as the concentration of Pd is increased, the adsorption of H_2 is also increased as evidenced by an increase in the ratio of total hydrogen uptake to CO adsorption. The limiting ratio of 3.33 obtained for silica-supported Pd is not approached until the composition of the supported bimetallic clusters has a relatively high concentration of Pd. In fact, the H_2/CO ratio remains constant over a fairly large concentration range. This suggests that the absorption of H_2 is inhibited in the case of Pt–Pd bimetallic clusters. It should be pointed out that the CO adsorption stoichiometry is also a function of surface composition. The concentration of bridging CO increases as the concentration of surface Pd atoms increases. The latter effect is small, however, and is expected to be well below the factor of 3 experimentally observed.

TABLE 1

The Effect of Surface Composition On the Adsorption of H_2 and CO On Silica-Supported Pt–Pd Bimetallic Clusters[a]

Pt/Pd	Co adsorbed (μmoles/g)	H_2 adsorbed (μmoles/g)	CO/M	H_2/CO	Reference
∞	—	—	—	0.5	(*20*)
4	49.42	39.85	0.15	0.81	
2	35.7	43.7	0.10	1.22	
1	68.6	82.7	0.16	1.21	
0.5	20.0	66.6	0.04	3.33	
0	53.74	178.6	0.12	3.33[b]	

[a] Total metal loading = 6%.
[b] Metal loading = 4.8%.

It is difficult to determine dispersions purely from CO and H_2 adsorption measurements in view of the complicating features associated with H_2 absorption and CO adsorption stoichiometry. The CO/M ratio may be taken as a rough measure of the relative dispersions of the bimetallic-cluster samples studied. It is interesting to observe that dispersions appear to be maximized when the concentrations of both metals are approximately equal.

In a previous study (*4*), it was observed that the exposure of a silica-supported Pt–Pd bimetallic cluster to an oxidizing atmosphere, followed by rereduction in hydrogen, induced the formation of Pd- and Pt-rich particles. We felt that it would be instructive to pursue this effect further by measuring the H_2/CO ratio as a function of repeated oxidation–reduction cycles. If Pd-rich particles are formed following each oxidation–reduction cycle, this ratio should increase due to enhanced H_2 absorption occurring over the Pd-rich particles. The results which are shown in Table 2 clearly shows this to be the case for a Pt–Pd (1 : 1) sample. Following three oxidation–reduction cycles, the H_2/CO ratio increased from 1.21 to 1.51 and the total H_2 uptake also increased significantly. The CO/M ratio decreased slightly, as expected, due to an increase in the adsorption of bridging CO over Pd-rich particles. The extent to which phase segregation has occurred following the three oxidation–reduction cycles is hard to determine in view of the sharp increase in the H_2/CO ratio which takes place between a Pt/Pd ratio of 1 and 0. A very rough extrapolation of the data, suggests that the surface composition has changed from an initial Pt/Pd ratio of 1 to

TABLE 2

The Effect of Successive Oxidation–Reduction Treatments on the Chemisorption of H_2 and CO on Silica-Supported Pt–Pd Bimetallic Clusters[a]

No. Oxidation–Reduction cycles	CO adsorbed (μmoles/g)	H_2 adsorbed (μmoles/g)	CO/M	H_2/CO
0	70.9	84.0	0.17	1.18
1	75.7	—	0.17	—
2	64.3	90.9	0.15	1.41
3	64.3	97.4	0.15	1.51

[a] Total metal loading = 6%, Pt/Pd = 1.

about 0.75 (Table 1). These experiments confirm the instability of silica-supported Pt/Pd bimetallic clusters in oxidizing environments and suggest the need to exclude oxygen if meaningful catalytic results are to be obtained on supported Pt–Pd bimetallic clusters.

Infrared Measurements

The chemisorption of CO on silica-supported Pt and Pd has been extensively studied by infrared spectroscopy. On silica-supported Pt, CO adsorbs only as a linear species to give a single intense infrared band centered at 2070 cm^{-1} (*5–8*). As shown in Fig. 1, CO adsorbed on Pd gives rise to two sets of infrared bands. The bands above 2000 cm^{-1} have been assigned to linearly bound CO and those below 2000 cm^{-1} have been assigned to bridge-bonded CO (*7, 15*). Blyholder (*16*) has challenged the latter assignment, pointing out that bands below 2000 cm^{-1} could be due to strongly backbonded, linearly bound CO occurring at Pd sites of low surface coordination. There is strong evidence, however, favoring the bridge-bonded model. When CO is adsorbed on PdO, the bands below 2000 cm^{-1} are no longer evident (*15*). This was explained by the 10% increase in the Pd–Pd distance in PdO, thus making bridging impossible. In a series of silica-supported Pd–Ag samples (*9*) and a series of silica-supported Pd–Au samples (*17*), it was found that as the mole fraction of the Group 1B metal was increased, the intensity of the lower-frequency bands relative to the higher-frequency bands decreased. A major reason for this was the decrease in the number of adjacent Pd atoms in the bimetallic samples.

As shown in Fig. 1, at full surface coverage bridged CO gives rise to a very intense band at 1980 cm^{-1} and a shoulder at 1900 cm^{-1}. Palazov *et al.* (*15*) have assigned the lower frequency shoulder to a purely bridge-bonded species (structure I) and the higher frequency band to a bridged species perturbed by a geminal, linearly adsorbed CO (structure II):

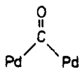

I

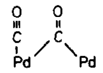

II

Their reasoning for the latter assignment is as follows: the linear and bridged species compete for electrons on Pd in order to fill their π^* orbitals. This results in less π^* electron density for the bridged species, causing an increase in the C–O bond order and a shift to a higher infrared frequency. In the light of more recent evidence, however, this assignment appears to be in error. Soma-Noto and Sachtler (*18*) have shown that the extinction coefficient for the linear CO species is 2 to 3 times greater than that of the bridged species. Thus, if structure II were correct, the intensity of the linear band should be at least 2 to 3 times greater than the intensity of the band at 1980 cm^{-1}. Clearly, from Fig. 1 and from previously published spectra (*5–7, 9, 15*), this is not the case.

There is another, more fundamental reason to question the above assignment. From the infrared frequency of the linearly adsorbed CO species, 2090 cm^{-1}, we see that this species experiences very little back bonding. In fact, the major electronic interaction between the linearly bound CO and the geminally shared Pd, is dative donation of an electron pair from CO to the surface Pd atom. The resulting increase in electron density on the Pd atom should therefore increase back bonding in the bridged species and cause a decrease in the infrared frequency.

Palazov *et al.* (*15*), and more recently, Kugler and Boudart (*17*) have presented convincing evidence that the observed shifts of frequency with coverage of the bridged bands are due to adsorbate–adsorbate interactions. The latter authors have also shown that an intense CO band centered at 1980 cm^{-1} seems to occur only on relatively large Pd particles. On very small particles this band is much smaller. Also, on a series of Pd–Ag samples (*9*), the intensity of the 1980 cm^{-1} band decreased relative to the 1900 cm^{-1} band as the percentage of Ag in the samples was increased. From a strictly geometric point of view, the formation of structure II should not be inhibited on small Pd particles or on Pd–Ag clusters. The relative intensities of the 1980 and 1900 cm^{-1} bands should, therefore, remain roughly constant on these systems. The fact that this is not the case argues against this assignment.

From the above considerations, a more reasonable adsorbate–adsorbate interaction might be that shown in structure III:

III

At low surface coverages, only the isolated bridge-bonded species (structure I) would be present. As the surface coverage is increased, the vicinal arrangement (structure III) would occur. This would result in a lower electron density on neighboring Pd atoms. Thus, less back bonding of the bridged CO would occur and the infrared frequency would increase. Structure III would also be less likely to occur on very small Pd particles and on Pd–Ag clusters. This should result in a lower intensity of the band at 1980 cm^{-1} relative to the 1900 cm^{-1} band. Subsequently, we shall refer to structure I as surface complex M2 and structure III as surface complex M1).

The stepwise adsorption and desorption of CO on a series of silica-supported Pt–Pd bimetallic-cluster samples of differing metallic composition are shown in Figs. 2–5. The bands above 2000 cm^{-1} are due to CO linearly adsorbed on Pt and Pd and those below 2000 cm^{-1} are due to CO bridge-bonded to Pd. The most striking feature of these spectra is that as the mole fraction of Pt is increased, the intensities of the bridged bands relative to the linear bands are decreased. The important intensities which must be considered, however, are those of the Pd–CO bridged bands relative to those of the Pd–CO linear bands. Intensities for the linear CO species on Pd are not easily obtained because these bands overlap the linear CO bands on Pt. Advantage

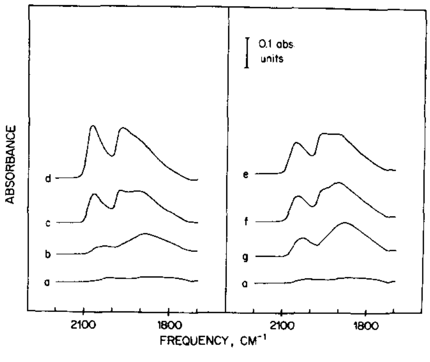

FIG. 2. Stepwise adsorption and desorption of CO on silica-supported Pt–Pd, total metal loading = 6%, 20 at.% Pt. (a) Background. (b) 1.4 × 10^{-2} Torr CO. (c) 0.22 Torr CO. (d) 15 Torr CO. (e) 2-min evacuation. $P = 3.1 \times 10^{-2}$ Torr. (f) 7-min evacuation. $P = 9.1 \times 10^{-3}$ Torr. (g) 1-hr evacuation. $P = 8.6 \times 10^{-4}$ Torr.

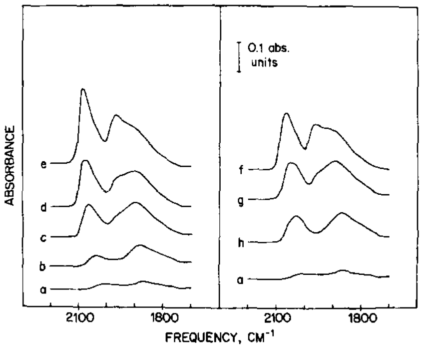

FIG. 3. Stepwise adsorption and desorption of CO on silica-supported Pt–Pd, total metal loading = 6%, 33 at.% Pt. (a) Background. (b) 7.7×10^{-3} Torr CO. (c) 4.8×10^{-2} Torr CO. (d) 0.73 Torr CO. (e) 19 Torr CO. (f) 1-min evacuation. $P = 0.22$ Torr. (g) 15-min evacuation. $P = 7.7 \times 10^{-3}$ Torr. (h) 1.5-hr evacuation. $P = 2.5 \times 10^{-4}$ Torr.

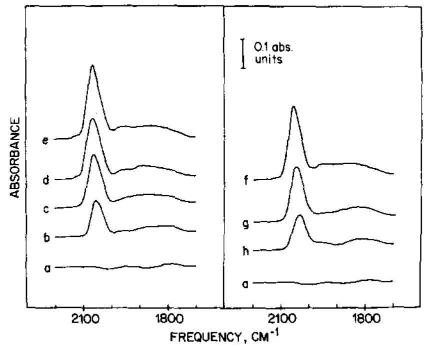

FIG. 5. Stepwise adsorption and desorption of CO on silica-supported Pt–Pd, total metal loading = 6%, 68 at.% Pt. (a) Background. (b) 2.6×10^{-2} Torr CO. (c) 0.95 Torr CO. (d) 12 Torr CO. (e) 23 Torr CO. (f) 1-min evacuation. $P = 0.30$ Torr. (g) 7-min evacuation. $P = 3.4 \times 10^{-3}$ Torr. (h) 3.5-hr evacuation. $P = 2.5 \times 10^{-5}$ Torr.

may be taken of the fact that linearly adsorbed CO on Pd is much more easily removed by evacuation than linearly adsorbed CO on Pt. It was determined that when the CO pressure was reduced to the 10^{-3}-Torr range, the residual linearly adsorbed CO on Pd could be neglected. Therefore, if the absorbance at the characteristic frequency is measured at full surface coverage and again after evacuation, the difference will give an accurate measure of the absorbance of linearly adsorbed CO on Pd at full surface coverage. The following procedure was used in computing the absorbance of CO linearly adsorbed on surface Pd atoms: the difference in absorbance at full surface coverage (P = 13–19 Torr), and after evacuation ($P = 3.9 \times 10^{-3}$ Torr), was determined at five wave number intervals over the range 2100 to 2070 cm^{-1}. The maximum difference was then taken to be the absorbance of CO linearly adsorbed on Pd and the frequency corresponding to the maximum was taken to be the frequency of the Pd–CO adsorption band. Using this technique, an average uncertainty in the frequency of about 2.5 cm^{-1} was expected. The value of the absorbance obtained in this way was considered adequate. The absorbance of linearly adsorbed CO on Pt was taken as the maximum of the band remaining in the linear region of the spectrum following evacuation.

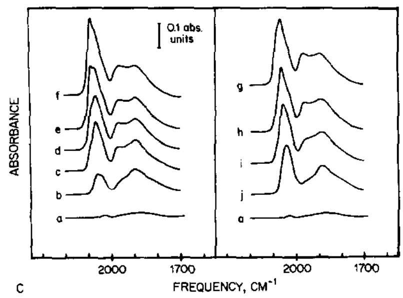

FIG. 4. Stepwise adsorption and desorption of CO on silica-supported Pt–Pd, total metal loading = 6%, 48 at.% Pt. (a) Background. (b) 5.4×10^{-3} Torr CO. (c) 8.6×10^{-2} Torr CO. (d) 0.54 Torr CO. (e) 3.3 Torr CO. (f) 13 Torr CO. (g) 1-min evacuation. $P = 0.22$ Torr. (h) 3-min evacuation. $P = 2.6 \times 10^{-2}$ Torr. (i) 8-min evacuation. $P = 3.4 \times 10^{-3}$ Torr. (j) 3.5-hr evacuation. $P < 1 \times 10^{-5}$ Torr.

The absorbance of the higher frequency band in the bridged region of the spectrum was also determined by the difference in absorbance at full surface coverage (P = 13 to 19 Torr) and after evacuation (10^{-4} to 10^{-5} Torr). The absorbance of the lower frequency band in the bridged region of the spectrum was detemined at full surface coverage. There are two reasons for this: (1) Fig. 1 shows that on pure Pd, the higher-frequency band is sharp and probably does not contribute very much to the absorbance of the lower-frequency band, and (2) upon evacuation, structure III is converted into structure I; that is, the intensity of the lower band increases following evacuation. These results are summarized in Table 3.

Considering structures I and III, it is evident that each bridged CO species "counts" two surface Pd atoms; similarly, each linear Pd–CO species "counts" one surface Pd atom. The total concentration of Pd atoms at the surface may then be expressed by Eq. (1), as follows:

$$(\mathrm{Pd})_s = 2(\mathrm{CO})_m + (\mathrm{CO})_l, \qquad (1)$$

where $(\mathrm{Pd})_s$ represents the total concentration of Pd surface atoms, $(\mathrm{CO})_m$ is the concentration of bridge-bonded CO, and $(\mathrm{CO})_l$ is the concentration of linearly adsorbed CO on Pd. In terms of absorbances and extinction coefficients Eq. (1) becomes:

$$(\mathrm{Pd})_s = \frac{2A_m}{k_m} + \frac{A_{\mathrm{Pd},l}}{k_l} = \frac{2(A_{ml} + A_{m2})}{k_m} + \frac{A_{\mathrm{Pd},l}}{k_l}, \qquad (2)$$

where A_{m1} and A_{m2} are the absorbances of complexes m1 and m2, respectively, and $A_{\mathrm{Pd},l}$ is the absorbance of linearly bound CO on Pd. The extinction coefficients for bridged and linear CO are given by k_m and k_l. The assumption is made that at the absorption maxima, $k_{m1} = k_{m2} = k_m$. Also, Soma-Noto and Sachtler have shown that the extinction coefficient of the linear adsorption complex is 2 to 3 times greater than that of the bridged (*10*, *18*). Setting $k_l = 2.5k_m$, Eq. (2) becomes,

$$(\mathrm{Pd})_s = \frac{5(A_{m1} + A_{m2}) + A_{\mathrm{Pd},l}}{2.5k_m} \qquad (3)$$

Since CO adsorbed on Pt exists only as a linear species, each linear CO on Pt "counts" one Pt surface atom:

$$(\mathrm{Pt})_s = (\mathrm{CO})_{\mathrm{Pt}} = A_{\mathrm{Pt}}/k_{\mathrm{Pt}}, \qquad (4)$$

where $(\mathrm{Pt})_s$ represents the concentration of surface Pt atoms, $(\mathrm{CO})_{\mathrm{Pt}}$ is the concentration of linearly absorbed CO on Pt, and A_{Pt} and k_{Pt} are the absorbance and extinction coefficient of this surface complex, respectively. Taking the ratio of surface Pt atoms to surface Pd atoms, Eq. (5) is obtained:

$$\frac{(\mathrm{Pt})_s}{(\mathrm{Pd})_s} + K\left[\frac{A_{\mathrm{Pt}}}{A_{\mathrm{Pd},l} + 5(A_{m1} + A_{m2})}\right], \qquad (5)$$

where $K = 2.5k_m/k_{\mathrm{Pt}}$. Thus, a plot of $[(\mathrm{Pt})_s/(\mathrm{Pd})_s]$ v_s $A_{\mathrm{Pt}}/[A_{\mathrm{Pd},l} + 5(A_{m1} + A_{m2})]$ should be linear and pass through the origin. We do not know $(\mathrm{Pt})_s$ and $(\mathrm{Pd})_s$ since the surface composition can be different form that of the bulk. However, if no surface enrichment occurs, a plot of the above function v_s the ratio of the bulk concentrations, (Pt)/(Pd), should also be linear. This Plot is shown in Fig. 6. The fact that this plot is linear is good evidence that the surface is not enriched in either metal.

It is apparent that the intensities of the bridged CO bands are depressed relative to the linear Pd–CO bands as the percentage of Pt is increased indicating the presence of

TABLE 3

Summary of Data for the Adsorption of CO over Supported Pt–Pd Bimetallic Clusters

X_{Pt}	$\frac{[\mathrm{Pt}]}{[\mathrm{Pd}]}$	A_{Pt}	Freq. (cm^{-1})	$A_{\mathrm{Pd},l}$	Freq. (cm^{-1})	A_{m1}	*Freq.* (cm^{-1})	A_{m2}	*Freq.* (cm^{-1})	$\frac{A_{\mathrm{Pt}}}{A_{\mathrm{Pd},l} + 5(A_{m1} + A_{m2})}$	$\frac{A_{\mathrm{Pd},l}}{A_{\mathrm{Pd},l} + A_{m1} + A_{m2}}$
0	0		—	0.13	2090	0.26	1980	0.12	1900	0	0.25
0.20	0.25	0.09	2050	0.15	2085	0.14	1970	0.12	1900	0.062	0.37
0.33	0.50	0.15	2050	0.26	2085	0.10	1965	0.10	1980	0.12	0.57
0.33	0.50	0.13	2050	0.25	2085	0.13	1960	0.11	1900	0.090	0.51
0.48	0.93	0.25	2060	0.23	2095	0.06	1960	0.09	1890	0.26	0.61
0.48	0.93	0.19	2060	0.23	2090	0.04	1960	0.09	1890	0.22	0.64
0.68	2.1	0.19	2045	0.12	2075	0.00	1960	0.06	1880	0.45	0.67

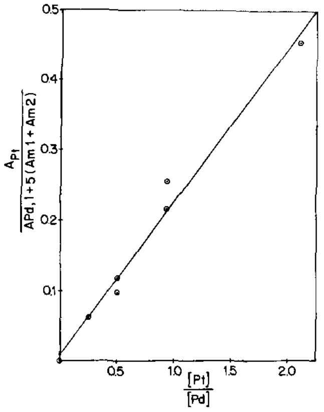

FIG. 6. Plot of $A_{Pt}/(A_{Pd,l} + (A_{m1} + A_{m2}))$ vs [Pt]/[Pd].

a geometric effect: multiple Pd atom sites are decreased in number, thereby reducing the amount of bridging which can occur. We must next consider whether geometric considerations are sufficient to account for the very large increase in the linear band intensities relative to the bridging CO bands or whether there is also a ligand effect involved.

In searching for an answer to this question, it is instructive to consider a theory developed by Sachtler (*10*). This theory is based on two primary assumptions: (1) the Pt atoms and Pd atoms are independently distributed on the surface; i.e., there is no short-range order, and (2) there are no electronic effects which favor the linear Pd–CO species over the bridged Pd–CO. Using these assumptions, an equation is derived in which $(X_{Pt})_s$, the mole fraction of Pt atoms on the surface, is plotted versus the function $A_{Pd,l}/[A_{Pd,l} + A_{m1} + A_{m2}]$. A plot using experimentally determined values may also be made. If the two plots agree, the above assumptions are justified. If the plots differ substantially, one or both of the assumptions must be incorrect.

The relationship derived by Sachtler (*10*), is shown in Eq. (6):

$$y = \frac{A_{Pd,l}}{A_{Pd,l} + A_{m1} + A_{m2}} = \frac{X_{Pt}{}^n + \lambda/P}{X_{Pt}{}^n(1-\lambda) + \lambda(P+1)/P}, \quad (6)$$

where $\lambda = \epsilon_m\theta_m/\epsilon_l\theta_l$ (ϵ_m and ϵ_l are the extinction coefficients for bridged and linear Pd–CO, and θ_m and θ_l are the fractional coverages of bridged and linear Pd–CO, respectively), $P = (A_{m1} + A_{m2}/A_{Pd,l})\, X_{Pt=0}$, and X_{Pt} is the mole fraction of Pt in the bulk. Actually, $(X_{Pt})_s$ should be used. However, since we have shown that there is no surface enrichment, it is justifiable to set $(X_{Pt})_s = X_{Pt}$.

In the present study, we have measured the absorbances of linear and bridged Pd–CO at full surface coverage; i.e., $\theta_m = \theta_l = 1$. Furthermore, we have assumed that $\epsilon_l = 2.5\epsilon_m$. Therefore, $\lambda = 1/2.5 = 0.40$. Also, from Table 1, $P = (0.26 + 0.12)/0.13 = 2.92$. Using these parameters and various values of n, a family of theoretical curves is shown in Fig. 7. Note that the initial slopes of these curves are all equal to zero, as required by differentiating (6):

$$\left(\frac{dy}{dX_{Pt}}\right)_{X_{Pt=0}} = 0. \quad (7)$$

The experimental plot is also shown in Fig. 7. Clearly, the experimental results differ substantially from theoretical predictions. Particularly significant is the fact that the experimental plot has a positive slope. It must be concluded, therefore, that either assumption (1), assumption (2), or both, are in error.

Our experimental curves in Fig. 7 are similar to those found by other workers on the Pd–Ag system (*10, 18, 19*). Sachtler (*10*) has shown that the disagreement of these curves from the calculated curves may be explained by a ligand effect which

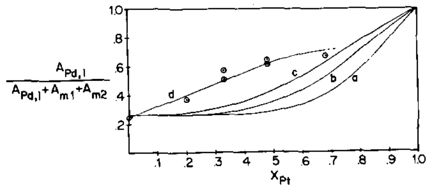

FIG. 7. Plots of $A_{Pd,l}/(A_{Pd,l} + A_{m1} + A_{m2})$. (a) Calculated curve assuming $\lambda = 0.40$ and $n = 6$. (b) Calculated curve, $\lambda = 0.40$, $n = 4$. (c) Calculated curve, $\lambda = 0.40$, $n = 3$. (d) Experimental curve.

favors the linear over the bridged Pd–CO species. In other words, by eliminating assumption (2), the calculated curves may be brought into agreement with the experimental curves. We shall now attempt to determine whether the experimental and calculated curves can be brought into agreement by eliminating assumption (1). In the following discussion, we assume that there is no ligand effect but we allow for the possibility of short-range ordering.

It was assumed in Ref. (*10*) that the conditional probability of having a Pd atom surrounded by n Pt atoms is given by $X_{\mathrm{Pt}}{}^{n}$. This assumes that the probability of occupancy of sites by Pt atoms is independent of whether the initial site is occupied by Pd or Pt. However, this is true only if the energies of Pt–Pd and Pd–Pd are equal; that is, it is true provided that there is no short-range ordering. This will occur only at temperatures well above an order–disorder transition or above a miscibility gap. We, therefore, replace the above conditional probability with:

$$P\,(\mathrm{Pd_{iso}}\,|\,\mathrm{Pd}) = X_{\mathrm{Pt}}{}^{n} + \Delta(X_{\mathrm{Pt}}), \tag{8}$$

where $P\,(\mathrm{Pd_{iso}}\,|\,\mathrm{Pd})$ is the conditional probability of an isolated Pd atom. Since $P\,(\mathrm{Pd_{iso}})$ must approach zero as X_{Pt} approaches zero:

$$\Delta(0) = 0. \tag{9}$$

For other X_{Pt}, $\Delta(X_{\mathrm{Pt}})$ will be positive if Pt next to Pd is favored (monophasic, ordered alloy) and negative if Pd next to Pd is favored (biphasic alloy) beyond what we would expect, assuming no correlation.

Substituting Eq. (8) in our expression for y, Eq. (6), we obtain,

$$\left(\frac{\partial y}{\partial X_{\mathrm{Pt}}}\right)_{X_{\mathrm{Pt}}=0} = \left[\frac{P^2}{\lambda(P+1)^2}\right]\left(\frac{\partial \Delta}{\partial X_{\mathrm{Pt}}}\right)_{X_{\mathrm{Pt}}=0} \tag{10}$$

for the initial slope of y vs X_{Pt}. From Eq. (10), it is observed that a positive initial slope may be explained by a positive $(\partial\Delta/\partial X_{\mathrm{Pt}})_{X_{\mathrm{Pt}}=0}$. This would imply a tendency for Pd atoms to prefer Pt neighbors, as in the case of systems which tend to form monophasic alloys. We conclude that a positive initial slope may be due to short-range ordering. Since Sachtler (*10*) has shown that a nonzero initial slope could also be due to a ligand effect, we cannot be sure whether our results are explained by an enhanced geometric effect due to short-range ordering, or whether they may be explained by a ligand effect. Indeed, they may be due to a combination of both. From a purely geometric point of view, y must always be greater than or equal to y_0. Therefore, an initial negative slope will always be indicative of a ligand effect.

Finally, from Table 3, we observe that the frequencies of most bands are decreased by 10–20 cm^{-1} on the bimetallic samples as compared to their monometallic counterparts (the frequency of CO linearly adsorbed on silica-supported Pt is 2070 cm^{-1}). This drop in frequency provides further evidence of the formation of bimetallic clusters. The drop in absorption frequency can be explained in terms of the coherent potential theory of alloy formation (*10*). According to this theory, the d bands of each metal in an alloy may remain separated, resulting in a decrease in the width of the d band with a corresponding increase in the density of electronic states. This would have the effect of increasing the availability of electrons for back bonding which, in turn, would weaken the strength of the CO bond. It would also discourage dative donation of electrons from CO to the metals.

CONCLUSIONS

Using simple mathematical arguments and infrared spectroscopy, we have detected no surface enrichment in either metal for a series of silica-supported Pt–Pd bimetallic clusters.

As the amount of Pt is increased, the intensities of the bands below 2000 cm^{-1} decrease relative to the linear CO band on Pd. This may be explained in part by a geometric effect whereby multiple Pd surface sites are decreased in number, thus providing fewer sites for bridging. Using arguments simlar to those used by Sachtler, we have concluded that a ligand effect which promotes the linearly adsorbed species over the bridge-bonded species on Pd may be operative. However, short-range ordering is also possible.

ACKNOWLEDGMENTS

Acknowledgment is made to the donors of the Petroleum Research Fund, administered by the American Chemical Society, for the support of this research. We also wish to acknowledge the National Science Foundation for the funds necessary to purchase a Perkin–Elmer model 281 Infrared Spectrometer under Grant DMR 78-18917.

REFERENCES

1. Hercules, D. M., *Anal. Chem.* **50**, 308 (1973).
2. Ramamoorthy, P., and Gonzalez, R. D., *J. Catal.* **58**, 188 (1979).
3. Grill, C. M., and Gonzalez, R. D., *J. Phys. Chem.* **84**, 878 (1980).
4. Grill, C. M., and Gonzalez, R. D., *J. Catal.* **64**, 487 (1980).
5. Eischens, R. P., Pliskin, W. A., and Francis, S. A., *J. Chem. Phys.* **22**, 1786 (1954).
6. Eischens, R. P., Pliskin, W. A., and Francis, S. A., *J. Phys. Chem.* **60**, 194 (1956).
7. Eischens, R. P., and Pliskin, W. A. *Advan. Catal.* **10**, 1 (1958).
8. Brown, M. F., and Gonzalez, R. D., *J. Catal.* **44**, 477 (1976).
9. Soma-Noto, Y., and Sachtler, W. M. H., *J. Catal.* **32**, 315 (1974).
10. Sachtler, W. M. H., *Catal. Rev. Sci. Eng.* **14**(2), 193 (1976).
11. Brown, M. F., and Gonzalez, R. D., *J. Phys. Chem.* **80**, 1731 (1976).
12. Ramamoorthy, P., Kosci, A., and Gonzalez, R. D., *J. Appl. Spectrosc.* **33**(31), 310 (1979).
13. Benson, J. E., Hwang, H. S., and Boudart, M. *J. Catal.* **30**, 146 (1973).
14. Aben, P. C., *J. Catal.* **10**, 224 (1968).
15. Palazov, A., Chang, C. C., and Kokes, R. J., *J. Catal.* **36**, 338 (1975).
16. Blyholder, G., *J. Phys. Chem.* **68**, 2772 (1964).
17. Kugler, E. L., and Boudart, M., *J. Catal.* **59**, 201 (1979).
18. Soma-Noto, Y., and Sachtler, W. M. H., *J. Appl. Phys. Suppl.* **2**, 241 (1974).
19. Primet, M., Mathieu, M. V., and Sachtler, W. M. H., *J. Catal.* **44**, 324 (1976).
20. Freel, J., *J. Catal.* **5**, 149 (1972).